Demonstration of the High Efficiency of an Air Plasma Jet Combining Electric Field and RONS in the Treatment of Chronic Wounds

Osvaldo Daniel Cortázar, Ana Megía-Macías, Bernardo Hontanilla, and Hernán Cortázar-Gallicchio

***Abstract*—A cold atmospheric air plasma jet (CAAPJ) for the treatment of skin injuries in medicine and veterinary medicine is presented with experimental evidence that point to the electric field inside the plasmas jet could be a determinant therapeutic mechanism. The device is characterized by producing a CAAPJ compatible with living tissues at a low-heat transfer rate with a temperature on the skin surface below 40 °C. It has a practical design to be used by physicians and veterinaries during daily practice, with a special focus on the treatment of skin injuries and unhealed ulcers. Plasma diagnostics, including currents-voltage signals, UV-VIS spectroscopy, IR images of the skin, and electric field measurements in the air cold plasma jet, are presented. The last is made for the first time in this type of plasma, and them can justify the induction of local electric currents on the wound surface to accelerate healing by highlighting the possible synergy with reactive oxygen and nitrogen species (RONSs) as a decontaminant agent for bacteria (including resistant), fungi and viruses without damaging healthy tissue. A remarkable clinical case study example is reported.**

***Index Terms*—Cold air atmospheric plasma jet (CAAPJ), plasma medicine, tissue regeneration ulcers, wound healing.**

Received 24 July 2024; revised 3 October 2024 and 21 October 2024; accepted 24 October 2024. Date of publication 28 October 2024; date of current version 5 May 2025. This work was supported in part by the Spanish Center of Development for Industrial Technology (CDTI. NEOTEC) under Program EXP-00104260/SNEO-20171007; in part by the Institute of Finance of Castilla-La Mancha, Spain (IFCLM, Adelante Program), under Contract 34; and in part by the COST Action PlasTHER "Therapeutical Applications of Cold Plasmas" under Grant CA20114, by the COST (European Cooperation in Science and Technology). *(Corresponding author: Osvaldo Daniel Cortázar.)*

This work involved human subjects or animals in its research. Approval of all ethical and experimental procedures and protocols was granted by the Spanish Agency of Drugs and Medical Devices (AEMPS) file 823/20/AE on 23 January 2020.

Osvaldo Daniel Cortázar is with the Mechanical Engineering Department, Superior Industrial School of Engineering, Comillas Pontifical University, 28840 Madrid, Spain (e-mail: odcortazar@comillas.edu).

Ana Megía-Macías is with the Mechanical Engineering Department, Superior Industrial School of Engineering, and the Institute of Technological Research, Comillas Pontifical University, 28840 Madrid, Spain (e-mail: ana.megia@comillas.edu)

Bernardo Hontanilla is with the Department of Plastic and Reconstructive Surgery, Clinica Universidad de Navarra, 31008 Pamplona, Spain (e-mail: bhontanill@unav.es).

Hernán Cortázar-Gallicchio is with the Multiprofessional Teaching Unit of Mental Health of the University Hospital Complex Insular Materno-Infantil, Canary Health Service, 35016 Las Palmas de Gran Canaria, Spain (e-mail: hcorgal@gobiernodecanarias.org).

Color versions of one or more figures in this article are available at https://doi.org/10.1109/TRPMS.2024.3486975.

Digital Object Identifier 10.1109/TRPMS.2024.3486975

I. Introduction

COLD atmospheric plasmas (CAPs) are increasingly popular in diverse applications, including medicine, veterinary medicine, agriculture, and food science [1], [2], [3], [4], [5], [6], [7]. The use of CAPs is supported by its efficacy as a decontaminant tool, the potential to promote wound healing, and the capacity to induce cancer cell death. Because they are highly unbalanced thermodynamically, they transfer a minimal amount of thermal energy to other bodies or materials. There is a general worldwide agreement that RONS administered by CAPs are successful in neutralizing bacteria, fungi, cancer cells, and viruses with a minimal impact on healthy tissue [8], [9], [10], [11], [12], [13], [14]. The active principle of oxidative stress generated by RONS is responsible for weakening microorganisms [15], [16], [17], [18], [19]. Mammalian cells possess a greater threshold for oxidative stress tolerance as compared to bacteria, fungi, and viruses due to their structural properties and stimulation of inherent self-repair mechanisms [20], [21], [22]. Although several research groups have contributed significantly to the development of cold atmospheric pressure plasma jets (CAAPJs) that can be used in direct contact with living tissues [23], [24], [25], [26], [27], in the device presented in this study, the air overheating has been solved by two patented innovations and its level of development is such that it can be used in hospitals by physicians and nurses in a practical and simple manner [28], [29], [30].

In addition, plasma diagnostics, comprising current-voltage signals and UV-VIS spectroscopy, are presented. Moreover, electric field measurements were performed on our *air* cold plasma jet. To the best of our knowledge, the measurements published so far were performed in Helium and Argon. We provide for the first time experimental evidence of electric field in this type of *air* plasma. This could justify the induction of local electrical currents at the wound surface as an important mechanism to accelerate healing, being the hypothesis that we will develop here.

II. Cold Air Plasma Jet Device

A CAAPJ device developed by the company MEDICAL PLASMAS [31], denominated PlasmAction Med, was used for the research described in this article. A general view photograph of the device is presented in Fig. 1 where its main components are indicated, and Fig. 2 shows a schematic block

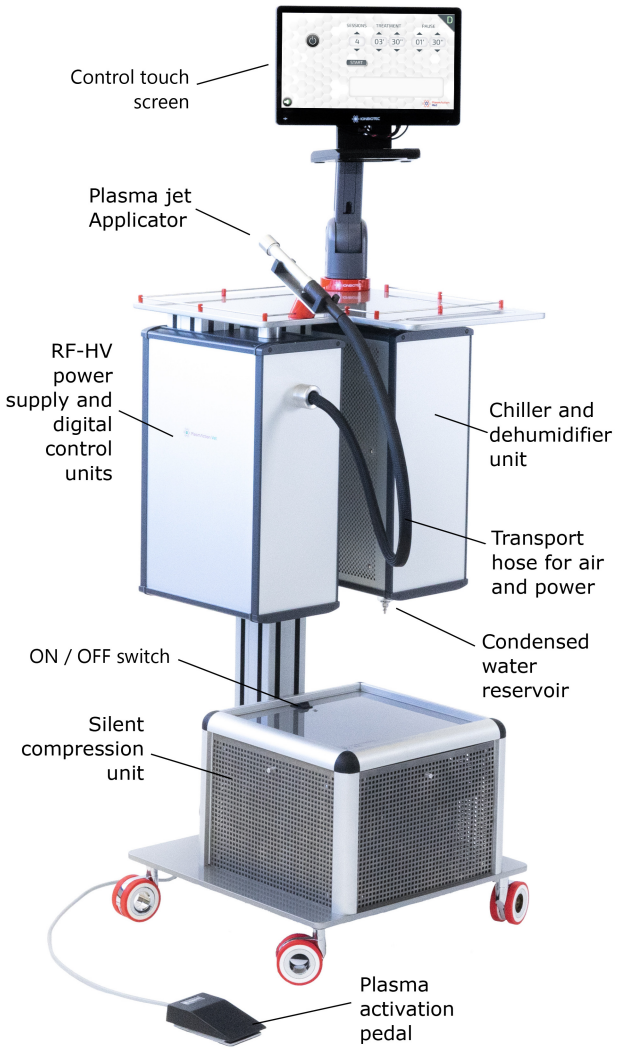

Fig. 1. General view of the plasma source device.

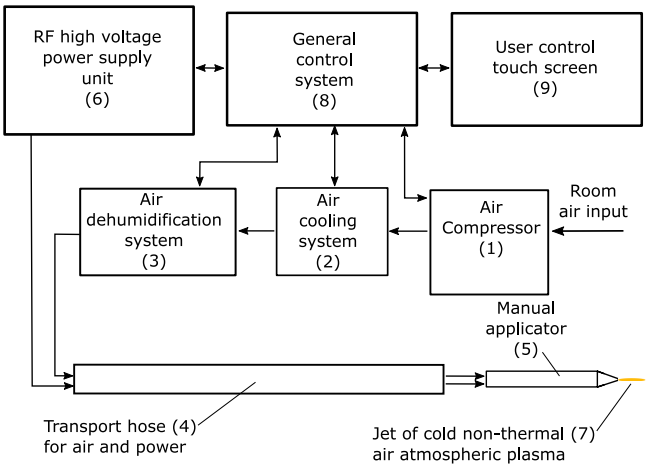

Fig. 2. Block diagram of the plasma source with subsystems.

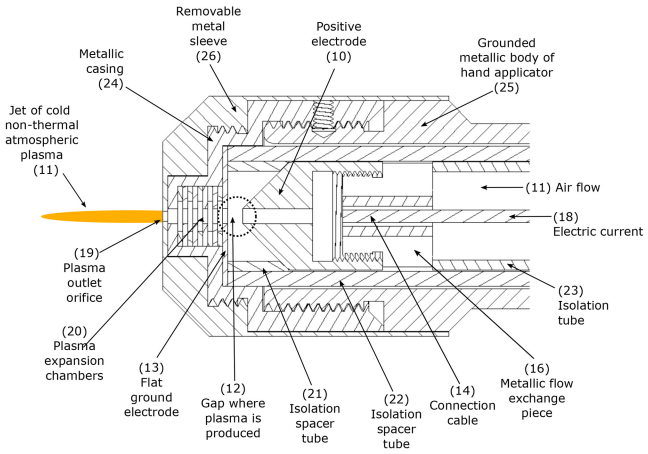

Fig. 3. Cross section of manual applicator head.

diagram with the interrelationship between subsystems. One silent diaphragm nonoil compressor (1) takes the room air and introduces a 10-l/min flow through the system. A first stage of cooling (2) reduces air temperature to by reaching 5 °C to 6 °C producing a water condensation (3) before injecting the flow into transport hose (4) to finally reach the manual applicator (5) where it is expelled. Once air flow reached a set of predetermined conditioning parameters, the high-voltage (HV) power supply of 15-kV RMS at 30 kHz (6) can be activated by means a the plasma activation pedal (see Fig. 1), so a plasma jet (7) is produced at the tip of manual applicator. The transport hose is a coaxial arrangement of a shielded HV cable and an external flexible silicon hose where electrical current flows in the center and air in the space between both. A build-in computer is in charge of the general control system (8) and interaction with the user is made by means of a touch screen (9) where treatment time and number of sessions can be set.

Fig. 3 shows a cross sectional view of the hand applicator tip where its structure is detailed and its main components are indicated by numbers in round brackets. The plasma discharge is produced between a pair of concentric and opposing electrodes separated by a gap of approximately 2 mm. Positive electrode (10) has a frustoconical shape with a passing-trough orifice from where air flow (11) is introduced in the gap where plasma is produced (12). The flat ground electrode (13) has a centered orifice that conducts to a series of plasma expansion chambers (14) composed by a stack of different alternating inner diameter washers. An output orifice of 2-mm diameter (19) determines the jet formation in the external atmosphere.

Inside of transport hose (4), the electrical current flows at center by a HV shielded cable and air around; but in the applicator this distribution must to be inverted by using the flow exchange piece (16). This is necessary in order to air flow (11) to pass through the hole in the center of the positive electrode (10) and establish the discharge in the gap between it and the flat ground electrode (13).

A removable sleeve made of stainless steel (26) covers the applicator head to prevent cross-contamination between patients through accidental direct contact of the applicator head with the wound surface during treatments.

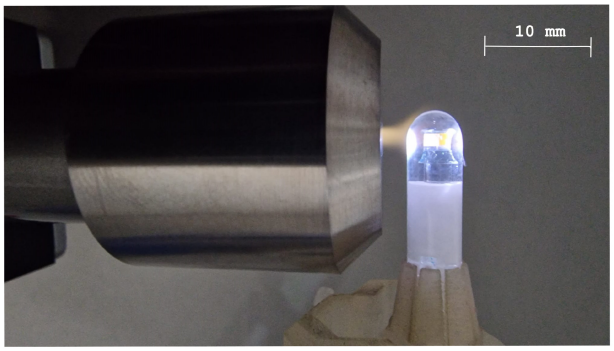

Fig. 4. Electric field electro-optical probe during a measure at 6 mm from the plasma nozzle.

III. Plasma Characterization

A. Electrical Characterization and Electric Field Measurement

The Voltage signal was measured with a HV probe by Tektronix model P6015A with a temporal response of 4 ns and a maximum rate of 40 kV of peak value. The current signal was measured with a TA189 current probe (Pico Technology) with a range between 2 mA and 30 A and 100-ns resolution. This is a clamp type inductive coil probe for scope measurements that was placed around the HV cable with a proper insulating centering piece at the output of HV power supply.

The electrical field in the sine of the cold air plasma jet was measured by using a electro-optical probe Kapteos, eoProbe with the Optic to Electro converter eoSense. This electro-optical system has a low permittivity ≈ 3.6, sensitivity 250 mV/m, up to 10 MV_{rms}/m, bandwidth 10 Hz to 12 GHz, spatial resolution of 1 mm according with data provided by the manufacturer. The probe is connected with an optical fiber cord to an interface (Kapteos, eoSense LF 100U-1) that convert the optical signal and voltage that can be recorded in a scope. The ET5-air is a Pockels effect-based probe that use the changes in a laser beam polarization produced by electric fields [32], [33], [34]. Fig. 4 shows a picture of the electro-optical probe during a measurement. The measurements of current, voltage and plasma electric field signals as a function of time were performed simultaneously. Fig. 5 shows the typical scope capture of the current (a), voltage (b) and electric field (c). HV and current probes were connected to the output of HV source that feeds the plasma generator while it is running showing that excitation is at 30 kHz with RMS voltage and current of 2.5 kV and 5 mA, respectively. The resulting RMS power delivered to the plasma is 15 W. However, it is important to note that the inductance of the secondary of the HV transformer and the capacitance of the coaxial cable and other components of the plasma jet applicator form an LC circuit that must be taken into account. In fact, we experimentally adjust the working frequency to match the resonant frequency $1/2\pi\sqrt{L.C}$ to make the transmission line losses negligible. Note that the current used to produce the plasma between the positive (10) and ground (13) electrodes shown in Fig. 3 has no direct relation to that which can be induced on the surface of a wound as we will discuss later in Section V.

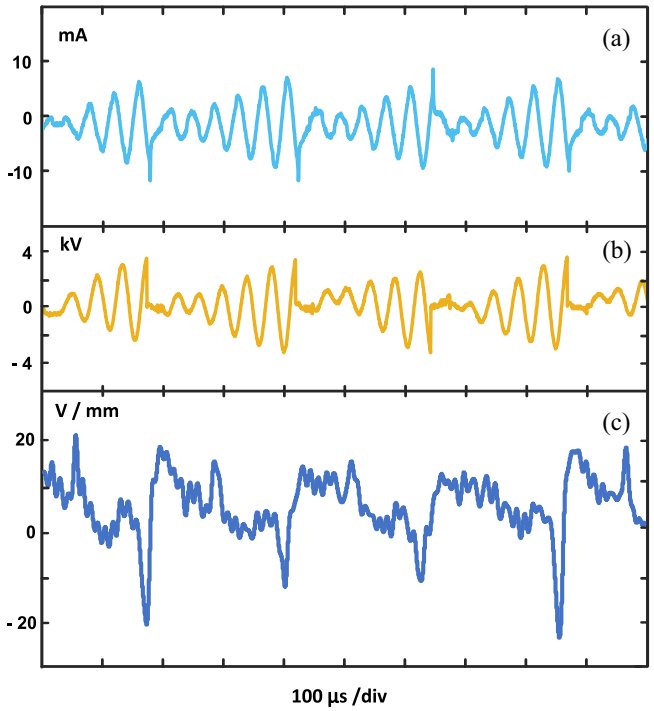

Fig. 5. Electric current intensity in the plasma jet (a) with RMS value of 5 mA, voltage (b) with RMS value of 2.5 kV and electric field signals (c) with peak values 20 V/mm.

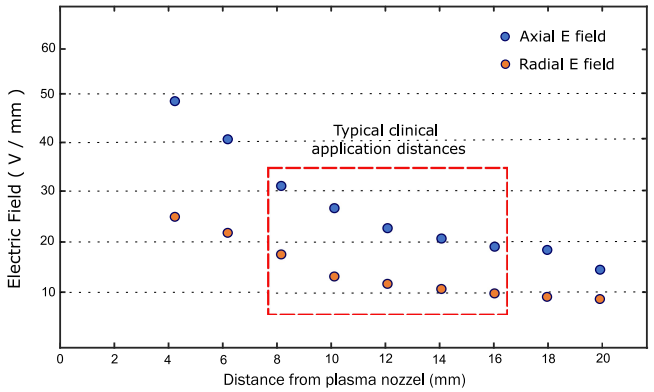

Fig. 6. Axial and radial plasma peak electric field versus distance from the applicator nuzzle.

The signal in Fig. 5(c) corresponds to a radial direction measurement at 6 mm of distance from plasma nozzle, as is shown in Fig. 4, and it follows current and voltage signals. In addition, the axial and radial components of the electric field were measured as a function of distance from the plasma jet output to determine its range. Fig. 6 illustrates such a spatial distribution where significant peak field values were detected up to a distance of 20 mm although the ones of more interest for us are those obtained from 8 to 16 mm because it is in the range where it is applied in the treatment of wounds. Observe that E-fields peak values from 10 to 30 V/mm are typical.

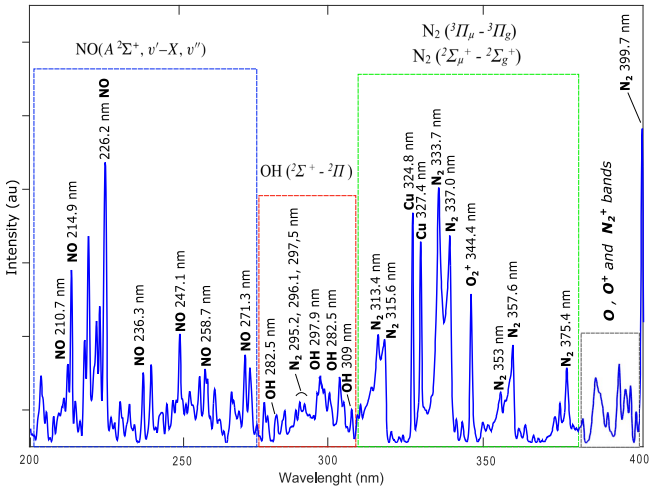

Fig. 7. UV spectrum from plasma jet in normal incidence from 200 to 400 nm.

B. UV Spectral Emission Measurements

Although only a few RONS can be observed by UV spectroscopy, it remains as a valuable tool for its simplicity and accessibility to observe the presence of important line groups associated to biological uses. Special attention is paid to UV range (200–400 nm) to observe the relative RONS abundance because its importance for biological applications. A fiber optics spectrometer from BWTEK Inc. Models Exemplar-LS BRC115P-U-UV (200–400 nm, resolution $\geq$ 0.6 nm) was use connected to an Ocean Insight model QP1000-2-SR (200–900 nm) fiber optics patch.

Fig. 7 shows a UV spectrum obtained at axial normal incidence (direct frontal) at 20-mm distance from the plasma nozzle, with a detailed molecular and radical emission from RONS like nitric oxide (NO), OH, and N_2 lines. The assignment of spectral lines in the spectrum of Fig. 7 has been carefully made taking into account the results of emission spectroscopy in CAPs by other authors published in a wide range of plasma generator devices [35], [36], [37], [38], [39], [40], [41].

We can see four packages of lines associated to molecular and atomic emissions that are inside of doted line boxes in the spectrum of Fig. 7. NO lines are mainly recorded between 200 and 280 nm from the molecular transition $A\,^2\Sigma^+,\ v' - X,\ v''$. Hydroxide anion ($HO^-$) lines are mainly recorded between 280 and 310 nm from the molecular transition $^2\Sigma^+ - {}^2\Pi$ with the exception of some molecular N_2 lines around 296 nm. The main emission package of N_2 lines is between 310 and 380 nm from molecular transition $^3\Pi_\mu - {}^3\Pi_g$ and $^2\Sigma_\mu^+ - {}^2\Sigma_g^+$. On the right side of the spectrum there an overlap of some O, O^+ and N_2^+ emission bands in the range of 380–400 nm is observed that cannot be resolved by our instrument [35], [39], [42], [43]. Moreover, two copper lines from the electrode contribution are also observed at 324.8 and 327.4 nm. The presence of NO lines between 200 and 280 nm is notable respect to other devices [44], [45], [46].

On the other hand, and considering the clinical application on living human and animal tissues, safety aspects are relevant. In this sense, we have paid special attention to the UV emission that can be projected on the tissue from the plasma jet because it could be a serious limitation for clinical application, as was opportunely observed by Nosenko et al. [47] for Argon jet devices. In addition, UV emission has been suggested as one of the physical decontamination factors in CAP devices and it must be resolved by measurements for our case [48]. To clarify this issue, a direct integrated measurement using a PCE Instruments UV radiometer and dosimeter model PCE-UV34 was used to measure the UV irradiance of the plasma source for safety monitoring with a resolution of 0.01 mW/cm^2 in a bandwidth of 260–390 nm and an accuracy of 4%. The radiometer was placed directly in front of the plasma jet at a distance of 10 mm at normal incidence of the detector surface. The obtained value is an upper limit of irradiance that does not take into account the sensitivity of living tissue to the different wavelengths as defined in Directive 2006/25/EC of the European Parliament and of the Council [49] where it can be seen that the weighted value will always be lower than that measured directly by the UV radiometer, which gives us an additional safety margin for the intended use of the CAP equipment used here. The peak value recorded with the radiometer was 0.074 W/m^2. Considering that the upper exposure limit established by the aforementioned directive is 30 J/m^2, then the maximum exposure time of the patient's skin to the UV emission of the plasma jet is 6.76 min. Taking into account that the treatment time never exceeds 1 min/cm^2, the observed area of illumination with normal incidence at 10-mm distance is 1.5 cm^2, the angle of incidence with which the plasma jet is applied to the surface is 45° and the above mentioned straight measurement of the radiometer, we can say with a wide safety margin that the use of this CAAPJ is safe.

C. Macroscopic Tissue Heating Effect

CAP jets are strongly out of thermodynamic equilibrium, however, once CAPs are interacting with some material a process of thermalization takes place and the measurement of temperature on the material surface makes sense as representative of its internal energy change ΔU. Moreover, in our specific case it is of great interest because it points directly on the use for which the device is intended.

An Optris PI640-640 $\times$ 480 pixels IR camera with a 12° $\times$ 9° IR microscope lens (f = 44 mm) was used to obtain the IR images. Fig. 8 shows two pictures showing the interaction between air plasma jet and a alive finger tip skin. Left image (a) is a visible picture and right (b) was taken by a IR camera. Note that the IR emission of the jet itself is not detected by the IR camera, only its effect on tissue surface is observed by temperature increasing. A doted line is superposed on the right picture to indicate the approximated jet dimensions. Maximum temperature in the skin is below 40 °C with no burning consequences on living tissue.

Our point of view for this analysis is macroscopic and it is based on the most recent review on the threshold of burn tissue damage in humans skin. It establishes that the perception of pain in the skin of an adult is just around 43 °C and that tissue damage occurs when 44 °C is exceeded [50]. Therefore, the

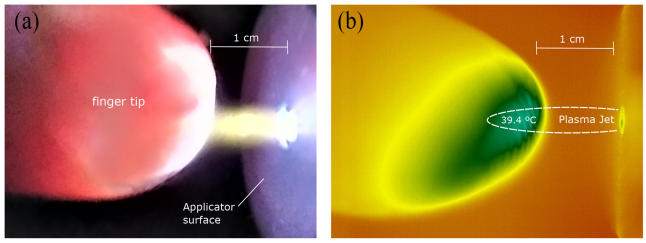

Fig. 8. Optical (a) and IR (b) pictures obtained during the interaction of air cold plasma jet with skin. IR emission form the jet can not be detected by IR camera until plasma touch the skin.

limit of 40 °C that we have established for ourselves is very prudent and is supported by our own evidence of the lack of discomfort and pain on the part of the patient during the entire treatment applied.

IV. Case Study—Use in Healing Torpid Ulcers

Preliminary medical tests have been carried out under the compassionate use protocol approved by the Spanish Agency of Drugs and Medical Devices (AEMPS) file 823/20/AE of 23 January 2020. A 94 years old female patient with previous pathologies of arterial hypertension due to arteriosclerosis, hypertensive heart disease, multifunctional anemia due to chronic disorder, folate deficiency and monoclonal gammopathy with ulcers in both feet was treated with the cold air plasma jet before described.

The protocol for preclinical treatment starts with a first stage where all tissue with necrosis is removed by scalpel and/or surgical scissors while full wound surface is cleaned with abundant saline solution and dried with sterile gauze. This operation is denominated debridement. After a final drying of the wound with a sterile gauze the cold air plasma jet is applied. The duration of each session was established depending of the wound surface, and this is calculated by using the criterion of 1 min/cm^2 of wound. Once the treatment is over, a sterile bandage is applied as usually in the wound cure. This protocol was repeated two times a week during nine weeks.

Fig. 9 shows a sequence of images with the evolution of an ulcer on the right foot instep from a surgical dehiscence associated with graft rejection where exposed tendons and bone without periosteum are observed. At the start of treatment, the ulcer had remained open for more than eight months with a poor prognosis, despite being treated regularly with a combination of pressure dressings and hydrocolloid patches.

Fig. 10 shows the sequence of same patient but with other torpid ulcer of 3 cm diameter on her left foot which reached one centimeter depth. During the first three weeks of treatment a decrease in inflammation, pain and redness was observed with a notable revascularization showing the formation of granular tissue. In subsequent weeks, tissue recovery occurred until complete closure in the ninth week.

V. Discussion

A new original equipment for the production of a cold air plasma jet which is intended for the treatment of chronic

Fig. 9. Sequence of pictures obtained during the compassionate treatment of a ulcer in a 92 years old patient.

Fig. 10. Sequence of pictures obtained during the compassionate treatment of a ulcer in a 92 years old patient.

wounds is presented, including electrical and plasma characterization measurements. A clinical case study on a patient with a negative prognosis of evolution after intensive testing of conventional treatments is also presented showing a remarkable result. In addition, first time electric field measurements within the air plasma jet induce us to consider its role as an important physical therapeutic mechanism.

The competition between physical and pharmacological effects of CAPs applied to wound healing acceleration is a current issue in the plasma medicine community. Kramer et al. [51] published a comprehensive review considering only the physical effects of heat transfer and UV

emission as decontamination agents in competition with the pharmacological decontaminant effect of RONS. In our case, both heat transfer and UV emission are too low to be seriously considered as is shown in Sections III-B and III-C. Another important reference has been made by Bekeschus et al. [52], where redox-based biochemistry is pointed out as the main driver of wound healing.

On the other hand, an important experimental evidence of the electric field produced in the sine of atmospheric plasma jets was recently published by Nastuta and Gerling [73] with a laboratory device of helium and argon jets. The values obtained range from 50 to 300 V/mm for helium and from 25 to 320 V/mm for argon. These fields were measured with a spatial resolution of 1 mm and a temporal resolution of ≤ 1 μs. The signals obtained show that the electric field wave follows the voltage and current waves generated by the plasma. Moreover, we have presented herein our own measurements using the same electro-optical probe system, which show a similar behavior of the V-I signals and with values of electric field ranging from 10 to 30 V/mm, as can be seen in Fig. 6.

An important question that emerges is whether these electric field values can be considered as being applied to the wound surface when the plasma interacts with the wound. For this we must take into account that these fields are time-varying following a waveform as shown in Fig. 5. This electric field wave is inevitably associated with a magnetic field wave (which we have not measured) which are indissoluble from each other according to Maxwell's equations. So, we can reduce the above question to the case of the interaction between this electromagnetic wave with a target surface and the consequences of this interaction on the values of both electric and magnetic fields.

For the case of a metal target [74], the charge carriers in the surface are free electrons that possess enormous mobility due to their small mass and the metal crystalline potential environment. These free electrons can react by canceling and reflecting any tangential electric field of an electromagnetic wave incident on the metal surface. The frequency response of these electrons to avoid penetration has a very wide range and reaches very high frequencies well above those used in plasma devices. In fact, this phenomenon is the basis of all passive electromagnetic shielding devices, such as the well-known Faraday's cage, as a classic example. The fact that the tangential transmitted electric field on the metal surface vanishes is well described by solving Maxwell's equations and is not surprising. Regarding the penetration of the normal components of the wave, it decays exponentially and its penetration will depend on the conductivity of material. However, the wave is capable of inducing surface currents that circulate in closed loops on the surface. This is how induction stoves and other devices work by Eddy currents regardless of whether they are grounded or not.

In contrast, when the target is an open wound the surface conditions are completely different. The wounds that are wet from their own exudative fluids present a surface with cells in liquid suspension and the presence of dissolved salts that allow both negative and positive molecular charge carriers to coexist in solution. Due to the size of these carriers and the medium in which they are found, its mobility is very low compared to the free electrons of a metal. Indeed, from a macroscopic point of view, this is observed with the appearance of an electrical resistance (measured in ohms) and the ability to cancel an external tangential electric field is very limited. In the case of dry chronic wounds these same physical arguments make the same behavior but even closer to a dielectric material where the tangential transmitted component of an external electric field remains intact, the penetration of normal components is deeper although the availability of carrier should be even lower. From these arguments, which can be verified in physics and chemistry textbooks, we consider that we can transfer the values measured in the plasma to the wound surface with considerable confidence.

TABLE I
ELECTRIC FIELDS VALUES THAT CAN BE DELIVERED ON A WOUND SURFACE BY WHESDS AND CAPJS: *Helium, Argon, and Air*

Device Type	Pulse duration (μs)	Electric Field (V/mm)
HVPC Wound Healing Electro Stimulator Devices [58]	50	1.5 -50
Cold Helium Plasma Jet [73]	60	50 - 300
Cold Plasma Argon Jet [73]	60	25 - 320
Cold Air Plasma Jet (See Fig. 5)	50	10 - 50

In addition to this, with no apparent link with CAPs, the effect of electric fields to accelerate wound healing has been clearly demonstrated by the well proven technology of wound healing electro-stimulation devices (WHESDs). WHESDs apply electric fields to unhealed wounds using a pair of electrodes attached to opposite edges of the wound and connected to a power source [53], [54], [55], [56], [57], [58], [59], [60], [61], [62]. There has been a wealth of literature on the benefits of accelerating wound healing using WHESD for over two decades, with positive results in accelerating the wound healing process by speeding up the migration of key cells [63] enhancing the migration of lymphocytes [64], fibroblasts [65], [66], [67], macrophages [68] and keratinocytes [69]. In fact, recent results in the use of electric fields for the regeneration of damaged tissue in spinal cord and transcranial lesions have been published by Matter et al. [70], Shaner et al. [71], and Lu [72]. The importance of electric fields in tissue regeneration processes has strong theoretical, experimental and clinical supporting evidence. For the specific case of chronic ulcers we are concerned with here, the typical parameters used by WHESD can be obtained from the work published by Kloth in 2014 [58]. The WHESD systems that are called HV pulsed current (HVPC) use short pulses of ≤ 50 μs and voltages ranging from 75-150 V with maximum values reaching 500 V. Given a typical ulcer size of 10 to 50 mm, the applied electric field can be easily estimated by dividing the applied voltage by the distance between the electrodes placed at the wound edges, giving values from 1.5 to 50 V/mm.

Table I shows the typical electric field values as they can be delivered on the wound surface in order to compare the technologies under discussion.

Unfortunately, we cannot directly measure the circulation of these induced currents, in contrast to WHESDs where the circulating current is easily measured because the wound is part of the circuit. However, the fact that the currents measured

with WHESDs exist, directly implies that the induced currents also exist because the physics involved is the Ohm's law, $\mathbf{j} = \sigma\mathbf{E}$ where $\mathbf{j}$ is the current density vector, σ the conductivity and $\mathbf{E}$ the electric field. So, the agreement showed in Table I between WHESD and the CAAPJs is significant because it implies the circulation of locally induced currents in the wound area where the jet is applied driven by the electric field and controlled by the local wound conductivity.

When a WHESD is used, the stagnation of wound healing is broken and the tissue reacts, showing a micro-revascularization that leads to a closure, with no doubt above that the breaking factor is the electric field. In the case of CAPs, the main mechanism of action that breaks the stagnation of chronic wounds in favor of a final closure remains under discussion. One extended explanation relates the biochemistry of nitric oxide (NO) with the angiogenesis observed in the tissue after plasma application [75], [76], [77]. However, the role of the electric field has been little mentioned, even in the case of dielectric barrier discharge (DBD) plasma devices, where its presence is evident [78], [79] and despite the fact that recent studies with DBD plasmas have shown that the improvement of microcirculation outlasts treatment time by measurements of oxygen saturation [80], [81], [82], [83]. But, on the other hand, we have deduced here that our cold plasma jets can induce currents in the same range as WHESD. Thus, the role of electric fields in helping to break stagnation in chronic wounds by stimulating microcirculation should be reviewed in the light of its possible synergy with the decontaminating selectivity of RONS. In our opinion, this synergy could explain the resounding success demonstrated by CAPs as a unique tool for the treatment of chronic wounds in medicine.

ACKNOWLEDGMENT

The authors wish to express their especial gratitude to Dr. Eduardo Pinés, Dr. María Carmen Ruíz Ruíz, Dr. Alba Gallego Torres, and Dr. Alberto Alía Miranda for their support during the initial veterinary tests with the first plasma source prototypes. The authors declare the following financial interests/personal relationships which may be considered as potential competing interests with the work reported in this article: Dr. Cortázar, Dr. Megía-Macías, and Dr. Hontanilla declare financial holdings in Medical Plasmas S. L. where they are co-founders and where the device used in this research was developed. Dr. Cortázar and Dr. Megía-Macías are also co-inventors of the cold air plasma jet device used in this research and authors of its corresponding European Unitary Patent EP3827878 entitled: "Electro-medical device for blood clotting and treatment of ulcers and other skin injuries in human and animal patients," granted on 7 June 2023; in Japan with N° JP7335958B2 granted on 30 September 2023; in China and Hong Kong with number CN112703034B granted on 30 April 2024 and in the USA with number US20210282832A1 granted on 28 May 2024 with the same title and authors.

AUTHOR CONTRIBUTIONS STATEMENT

1) *Conceptualization:* ODC and AMM.
2) *Methodology:* ODC, AMM, BH, and HCG.
3) *Investigation:* ODC, AMM, BH, and HCG.
4) *Resources:* ODC, AMM, and BH.
5) *Writing–Original Draft:* ODC.
6) *Writing, Review, and Editing:* ODC, AMM, BH, and HCG.

REFERENCES

[1] A. Fridman, *Plasma Science and Technology*. Weinheim, Germany: Wiley, 2024.
[2] A. Fridman and G. Friedman, *Plasma Medicine*. New York, NY, USA: Wiley, 2013.
[3] M. Laroussi, "Sterilization of contamined matter with atmospheric pressure plasma," *IEEE Trans. Plasma Sci.*, to be published.
[4] M. Laroussi, M. Kong, G. Morfill, and W. Stolz, *Plasma Medicine: Applications of Low Temperature Gas Plasmas in Medicine and Biology*. Cambridge, U.K.: Cambridge Univ. Press, 2012.
[5] I. Adamovich et al., "The 2017 plasma roadmap: Low temperature plasma science and technology," *J. Phys. D, Appl. Phys.*, vol. 50, Jul. 2017, Art. no. 323001.
[6] T. V. Woedtke, A. Schmidt, S. Bekeschus, K. Wende, and K. D. Weltmann, "Plasma medicine: A field of applied redox biology," *In Vivo*, vol. 33, no. 4, pp. 1011–1026, 2019.
[7] D. B. Graves, "Low temperature plasma biomedicine: A tutorial review," *Phys. Plasmas*, vol. 21, Aug. 2014, Art. no. 080901.
[8] P. Shaw et al., "Bacterial inactivation by plasma treated water enhanced by reactive nitrogen species," *Sci. Rep.*, vol. 8, p. 12 Jul. 2018.
[9] S. Suwal, C. P. Coronel-Aguilera, J. Auer, B. Applegate, A. L. Garner, and J. Y. Huang, "Mechanism characterization of bacterial inactivation of atmospheric air plasma gas and activated water using bioluminescence technology," *Innov. Food Sci. Emerg. Technol.*. vol. 53, pp. 18–25, May 2019. [Online]. Available: https://doi.org/10.1016/j.ifset.2018.01.007
[10] C. M. Lin, Y. C. Chu, C. P. Hsiao, J. S. Wu, C. W. Hsieh, and C. Y. Hou, "The optimization of plasma-activated water treatments to inactivate *SalmonellaEnteritidis* (ATCC 13076) on shell eggs," *Foods*, vol. 8, no. 10, p. 520, 2019.
[11] S. Takeda et al., "Intraperitoneal administration of plasma-activated medium: Proposal of a novel treatment option for peritoneal metastasis from gastric cancer," *Ann. Surg. Oncol.*, vol. 24, no. 5, pp. 1188–1194, 2017.
[12] E. Turrini et al., "Plasma-activated medium as an innovative anticancer strategy: Insight into its cellular and molecular impact on in vitro leukemia cells," *Plasma Process. Polym.*, vol. 17, pp. 1–14, Oct. 2020.
[13] C. Canal, R. Fontelo, I. Hamouda, J. Guillem-Marti, U. Cvelbar, and M. P. Ginebra, "Plasma-induced selectivity in bone cancer cells death," *Free Rad. Biol. Med.*, vol. 110, pp. 72–80, Sep. 2017. [Online]. Available: http://dx.doi.org/10.1016/j.freeradbiomed.2017.05.023
[14] M. Mateu-Sanz et al., "Cold plasma-treated ringer's saline: A weapon to target osteosarcoma," *Cancers*, vol. 12, pp. 1–19, Jan. 2020.
[15] P. marie Girard, A. Arbabian, M. Fleury, G. Bauville, V. Puech, M. Dutreix, and J. S. Sousa, "Synergistic effect of H_2O_2 and NO_2 in cell death induced by cold atmospheric He plasma," *Sci. Rep.*, vol. 6, pp. 1–17, Jul. 2016. [Online]. Available: http://dx.doi.org/10.1038/srep29098
[16] G. Bauer, D. Sersenová, D. B. Graves, and Z. Machala, "Dynamics of singlet oxygen-triggered, RONS-based apoptosis induction after treatment of tumor cells with cold atmospheric plasma or plasma-activated medium," *Sci. Rep.*, vol. 9, p. 12, Sep. 2019.
[17] G. Bauer, "The synergistic effect between hydrogen peroxide and nitrite, two long-lived molecular species from cold atmospheric plasma, triggers tumor cells to induce their own cell death," *Redox Biol.*, vol. 26, Sep. 2019, Art. no. 101291. [Online]. Available: https://doi.org/10.1016/j.redox.2019.101291
[18] X. Liao, D. Liu, Q. Xiang, J. Ahn, S. Chen, X. Ye, and T. Ding, "Inactivation mechanisms of nonthermal plasma on microbes: A review," *Food Control*, vol. 75, pp. 83–91, May 2017. [Online]. Available: http://dx.doi.org/10.1016/j.foodcont.2016.12.021
[19] R. Zhou, R. Zhou, K. Prasad, Z. Fang, R. Speight, K. Bazaka, and K. Ostrikov, "Cold atmospheric plasma activated water as a prospective disinfectant: The crucial role of peroxynitrite," *Green Chem.*, vol. 20, no. 23, pp. 5276–5284, 2018.
[20] K. Apel and H. Hirt, "Reactive oxygen species: Metabolism, oxidative stress, and signal transduction," *Annu. Rev. Plant Biol.*, vol. 55, no. 1, pp. 373–399, Jan. 2004.

[21] J. D. Hayes, A. T. Dinkova-Kostova, and K. D. Tew, "Oxidative stress in cancer," *Cancer Cell*, vol. 38, pp. 167–197, Aug. 2020. [Online]. Available: https://doi.org/10.1016/j.ccell.2020.06.001

[22] K. P. Loh, S. H. Huang, R. D. Silva, B. K. H. Tan, and Y. Z. Zhu, "Oxidative stress: Apoptosis in neuronal injury," *Curr. Alzheimer Res.*, vol. 3, pp. 327–337, Sep. 2006.

[23] J. F. Kolb et al., "Cold atmospheric pressure air plasma jet for medical applications," *Appl. Phys. Lett.*, vol. 92, pp. 23–25, Jun. 2008.

[24] Y. C. Hong and H. S. Uhm, "Air plasma jet with hollow electrodes at atmospheric pressure," *Phys. Plasmas*, vol. 14, May 2007, Art. no. 053503.

[25] M. H. Chiang, J. Y. Wu, Y. H. Li, J. S. Wu, S. H. Chen, and C. L. Chang, "Inactivation of *E.coli* and *B.subtilis* by a parallel-plate dielectric barrier discharge jet," *Surf. Coat. Technol.*, vol. 204, pp. 3729–3737, Aug. 2010.

[26] L. Chen, Y. Wei, X. Zuo, J. Cong, and Y. Meng, "The atmospheric pressure air plasma jet with a simple dielectric barrier," vol. 521, pp. 226–228, Oct. 2012.

[27] X. Lu, D. Liu, Y. Xian, L. Nie, Y. Cao, and G. He, "Cold atmospheric-pressure air plasma jet: Physics and opportunities," vol. 28, Oct. 2021, Art. no. 100501.

[28] O. Cortázar and A. Megía-Macías, "Electromedical device for blood clotting and treatment of ulcers and other skin injuries in human and animal patients," Unitary European Patent EP3 827 878, Jul. 2023.

[29] O. D. Cortázar and A. Megía-Macías, "Electromedical device for blood clotting and treatment of ulcers and other skin injuries in human and animal patients," Japan Patent JP7 335 958 B2, Sep. 2023.

[30] O. D. Cortázar and A. Megía-Macías, "Electromedical device for blood clotting and treatment of ulcers and other skin injuries in human and animal patients," China Patent CN 11 270 303 4B, Apr. 2024.

[31] [Online]. Available: www.medicalplasmas.com

[32] M. Bernier, G. Gaborit, L. Duvillaret, A. Paupert, and J. L. Lasserre, "Electric field and temperature measurement using ultra wide bandwidth pigtailed electro-optic probes," *Appl. Opt.*, vol. 47, no. 13, pp. 2470–2476, 2008.

[33] G. Gaborit, S. Reuter, S. Iseni, and L. Duvillaret, "Cold plasma diagnostic using vectorial electrooptic probe," in *Proc. 5th Int. Conf. Plasma Med.*, 2014, p. 1.

[34] G. Gaborit et al., "Single shot and vectorial characterization of intense electric field in various environments with pigtailed electrooptic probe," *IEEE Trans. Plasma Sci.*, vol. 42, pp. 1265–1273, May 2014.

[35] A. M. Bass, H. P. Broida, "A spectrometric atlas of the $^2\Sigma^+$–$^2\Pi$ transition of OH," Nat. Bureau Stand., Gaithersburg, MD, USA, Rep. 541, 1953.

[36] F. Liu, W. Wang, C. Li, W. Zheng, and Y. Wang "Diagnosis of OH radical by optical emission spectroscopy in a wire-plate bi-directional pulsed corona discharge," *Journal of Electrostatics*, Vol. 65, 2007.

[37] J. N. Misra, D. Ziuzina, P. J. Cullen, and K. M. Keener "Characterization of a novel atmospheric air cold plasma system for treatment of biomaterials," *Trans. ASABE*, Vol. 53, no. 3, pp. 1011–1016, 2013.

[38] L. Giuliani, J. J. Gallego, F. Minotti, H. Kelly, and D. Grondona "Emission spectroscopy of an atmospheric pressure plasma jet operated with air at low frequency," *J. Phys., Conf. Ser.*, vol. 591, Mar. 2015, Art. no. 012048.

[39] N. Bolouki, J. hsing Hsieh, C. Li, and Y. zheng Yang, "Emission spectroscopic characterization of a helium atmospheric pressure plasma jet with various mixtures of argon gas in the presence and the absence of de-ionized water as a target," *Plasma*, vol. 2, no. 3, pp. 283–293, 2019.

[40] J. Mrotzek, and W. Viöl "Spectroscopic characterization of an atmospheric pressure plasma jet used for cold plasma spraying," *Appl. Sci.*, Vol. 12, no. 13, p. 6814, 2022.

[41] J. Jaiswal, E. M. Aguirre, and G. Veda-Prakash "A KHz frequency cold atmospheric pressure argon plasma jet for the emission of $O(^1S)$ auroral lines in ambient air," *Sci. Rep.*, Vol. 11, p. 1893, Jan. 2021.

[42] J. Golda and J. Benedikt, "Vacuum ultraviolet spectroscopy of cold atmospheric pressure plasma jets plasma source," *Plasma Process. Polym.*, vol. 17, no. 6, pp. 1–12, Jan. 2020.

[43] P. Thana et al., "A compact pulse-modulation cold air plasma jet for the inactivation of chronic wound bacteria: Development and characterization," *Heliyon*, vol. 5, Sep. 2019, Art. no. e02455. [Online]. Available: https://doi.org/10.1016/j.heliyon.2019.e02455

[44] M. S. Mann et al., "Introduction to DIN-specification 91315 based on the characterization of the plasma jet kiNPen® MED," *Clin. Plasma Med.*, vol. 4, pp. 35–45, Dec. 2016. [Online]. Available: http://dx.doi.org/10.1016/j.cpme.2016.06.001

[45] F. do Nascimento, S. Moshkalev, and M. Machida, "Changes in properties of dielectric barrier discharge plasma jets for different gases and for insulating and conducting transfer plates," *Braz. J. Phys.*, vol. 47, pp. 278–287, Mar. 2017.

[46] S. Reuter, T. V. Woedtke, and K. D. Weltmann, "The kiNPen—A review on physics and chemistry of the atmospheric pressure plasma jet and its applications," *J. Phys. D, Appl. Phys.*, vol. 51, May 2018, Art. no. 233001.

[47] T. Nosenko, T. Shimizu, J. Zimmermann, B. Steffes, and G. E. Morfill, "Argon plasma vs. air plasma: Characteriazation and interaction with biological systems," in *Proc. IEEE Int. Conf. Plasma Sci.*, 2010, pp. 1–29.

[48] T. Bernhardt, M. L. Semmler, M. Schäfer, S. Bekeschus, S. Emmert, and L. Boeckmann, "Plasma medicine: Applications of cold atmospheric pressure plasma in dermatology," *Oxidat. Med. Cell. Longev.*, vol. 2019, pp. 10–13, Sep. 2019.

[49] *Directive 2006/25/EC European Parliament and the Council*, European Union, Luxembourg City, Luxembourg, Apr. 2006.

[50] N. A. Martin, M. Falder, "A Review of the evidence for threshold of burn injury," *Burns*, vol.43, pp. 1624–1639, Dec. 2017.

[51] A. Kramer et al., "Cold atmospheric pressure plasma for treatment of chronic wounds: Drug or medical device?" *J. Wound Care*, vol. 26, pp. 470–475, Aug. 2017.

[52] S. Bekeschus, T. von Woedtke, S. Emmert, and A. Schmidt, "Medical gas plasma-stimulated wound healing: Evidence and mechanisms: Mechanisms of gas plasma-assisted wound healing," *Redox Biology*, vol. 46, Oct. 2021, Art. no. 102116. [Online]. Available: https://doi.org/10.1016/j.redox.2021.102116

[53] S. E. Gardner, R. A. Frantz, and F. L. Schmidt, "Effect of electrical stimulation on chronic wound healing: A meta- analysis," *Wound Repair Regenerat.*, vol. 7, pp. 495–503, Nov./Dec. 1999.

[54] R. Nuccitelli, "A role for endogenous electric fields in wound healing," *Curr. Topics Develop. Biol.*, vol. 58, no. 2, pp. 1–26, 2003.

[55] B. Song, M. Zhao, J. Forrester, and C. McCaig, "Nerve regeneration and wound healing are stimulated and directed by an endogenous electrical field in vivo," *J. Cell Sci.*, vol. 117, no. 20, pp. 4681–4690, 2004.

[56] L. C. Kloth, "Electrical stimulation for wound healing: A review of evidence from in vitro studies, animal experiments, and clinical trials," *Int. J. Lower Extrem. Wounds*, vol. 4, pp. 23–44, Mar. 2005.

[57] G. Thakral, J. LaFontaine, B. Najafi, T. K. Talal, P. Kim, and L. A. Lavery, "Electrical stimulation to accelerate wound healing," *Diabet. Foot Ankle*, vol. 4, no. 1, Sep. 2013, Art. no. 22081.

[58] L. C. Kloth, "Electrical stimulation technologies for wound healing," *Adv. Wound Care*, vol. 3, no. 2, pp. 81–90, 2014.

[59] B. Reid and M. Zhao, "The electrical response to injury: Molecular mechanisms and wound healing," *Adv. Wound Care*, vol. 3, no. 2, pp. 184–201, 2014.

[60] G. Tai, M. Tai, and M. Zhao, "Electrically stimulated cell migration and its contribution to wound healing," *Burns Trauma*, vol. 6, pp. 1–7, 2018.

[61] R. Luo, J. Dai, J. Zhang, and Z. Li, "Accelerated skin wound healing by electrical stimulation," *Adv. Healthc. Mater.*, vol. 10, pp. 1–15, May 2021.

[62] S. B. Rajendran, K. Challen, K. L. Wright, and J. G. Hardy, "Electrical stimulation to enhance wound healing," *J. Funct. Biomater.*, vol. 12, no. 2, p. 40, 2021.

[63] M. Zhao et al., "Electrical signals control wound healing through phosphatidylinositol-3-OH kinase-gamma and PTEN," *Nature*, vol. 442, pp. 457–460, Jul. 2006.

[64] F. Lin et al., "Lymphocyte electrotaxis in vitro and in vivo," *J. Immunol.*, vol. 181, pp. 2465–2471, Aug. 2008.

[65] M. Sugimoto et al., "Optimum microcurrent stimulation intensity for galvanotaxis in human fibroblasts," *J. Wound Care*, vol. 21, nos. 5–6, pp. 5–9, 2015.

[66] G. J. Bourguignon and L. Y. W. Bourguignon, "Electric stimulation of protein and DNA synthesis in human fibroblasts," *FASEB J.*, vol. 1, pp. 398–402, Nov. 1987.

[67] G. J. Bourguignon, W. Jy, and L. Y. W. Bourguignon, "Electric stimulation of human fibroblasts causes an increase in ca2+ influx and the exposure of additional insulin receptors," *J. Cell. Physiol.*, vol. 140, pp. 379–385, Aug. 1989.

[68] N. Orida and J. D. Feldman, "Directional protrusive pseudopodial activity and motility in macrophages induced by extracellular electric fields," *Cell Motil.*, vol. 2, no. 3, pp. 243–255, 1982.

[69] K. Y. Nishimura, R. R. Isseroff, and R. Nucciteili, "Human keratinocytes migrate to the negative pole in direct current electric fields comparable to those measured in mammalian wounds," *J. Cell Sci.*, vol. 109, pp. 199–207, Jun. 1996.

[70] L. Matter, B. Harland, B. Raos, D. Svirskis, and M. Asplund, "Generation of direct current electrical fields as regenerative therapy for spinal cord injury: A review," *APL Bioeng.*, vol. 7, no. 3, Sep. 2023, Art. no. 031505.

[71] S. Shaner et al., "Bioelectronic microfluidic wound healing: A platform for investigating direct current stimulation of injured cell collectives," *Lab Chip*, vol. 23, pp. 1531–1546, Jan. 2023.

[72] H. Lu, S. Shaner, E. Otte, M. Asplund, and A. Vlachos, "A microfluidic perspective on conventional in vitro transcranial direct current stimulation methods," *J. Neurosci. Methods*, vol. 385, Feb. 2023, Art. no. 109761.

[73] A. V. Nastuta and T. Gerling, "Cold atmospheric pressure plasma jet operated in Ar and He: From basic plasma properties to vacuum ultraviolet, electric field and safety thresholds measurements in plasma medicine," *Appl. Sci.*, vol. 12, p. 644, Jan. 2022.

[74] T. Darny, J-M. Pouvesle, C. Douat, S. Dozias, and E. Robert, "Analysis of conductive target influence in plasma jet experiments through helium metastable and electric field measurements," *Plasma Sources Sci. Technol.*, vol. 26, Mar. 2017, Art. no. 045008.

[75] C. Duchesne, S. Banzet, J. Lataillade, A. Rousseau, and N. Frescaline, "Cold atmospheric plasma modulates endothelial nitric oxide synthase signalling and enhances burn wound neovascularisation," *J. Pathol.*, vol. 249, no. 3, pp. 368–380, 2019.

[76] S. Fathollah et al., "Investigation on the effects of the atmospheric pressure plasma on wound healing in diabetic rats," *Sci. Rep.*, vol. 6, Feb. 2016, Art. no. 19144.

[77] K. Heuer et al., "The topical use of nonthermal dielectric barrier discharge (DBD): Nitric oxide related effects on human skin," *Nitr. Oxide Biol. Chem.*, vol. 44, pp. 52–60, Jan. 2015. [Online]. Available: http://dx.doi.org/10.1016/j.niox.2014.11.015

[78] K. P. Arjunan and A. M. Clyne, "Hydroxyl radical and hydrogen peroxide are primarily responsible for dielectric barrier discharge plasma-induced angiogenesis," *Plasma Process. Polym.*, vol. 8, pp. 1154–1164, Dec. 2011.

[79] K. P. Arjunan, G. Friedman, A. Fridman, and A. M. Clyne, "Nonthermal dielectric barrier discharge plasma induces angiogenesis through reactive oxygen species," *J. Royal Soc. Interface*, vol. 9, pp. 147–157, Jan. 2012. [Online]. Available: https://royalsocietypublishing.org/doi/10.1098/rsif.2011.0220

[80] T. Kisch et al., "The repetitive use of nonthermal dielectric barrier discharge plasma boosts cutaneous microcirculatory effects," *Microvasc. Res.*, vol. 106, pp. 8–13, Jul. 2016. [Online]. Available: http://dx.doi.org/10.1016/j.mvr.2016.02.008

[81] T. Kisch et al., "Improvement of cutaneous microcirculation by cold atmospheric plasma (CAP): Results of a controlled, prospective cohort study," *Microvasc. Res.*, vol. 104, pp. 55–62, Mar. 2016. [Online]. Available: http://dx.doi.org/10.1016/j.mvr.2015.12.002

[82] J. O. Jensen et al., "The repetitive application of cold atmospheric plasma (CAP) improves microcirculation parameters in chronic wounds," *Microvasc. Res.*, vol. 138, Nov. 2021, Art. no. 104220. [Online]. Available: https://doi.org/10.1016/j.mvr.2021.104220

[83] N. Matzkeit et al., "Cold atmospheric plasma improves cutaneous microcirculation in standardized acute wounds: Results of a controlled, prospective cohort study," *Microvasc. Res.*, vol. 138, Nov. 2021, Art. no. 104211.